Archived at the Flinders Academic Commons:

http://dspace.flinders.edu.au/dspace/

"This is the peer reviewed version of the following article:

Yu, L., Tune, D.D., Shearer, C.J. and Shapter, J.G., 2015. Heterojunction solar cells based on silicon and composite films of graphene oxide and carbon nanotubes. ChemSusChem, 8(17), 2940-2947, which has been published in final form at:

http://onlinelibrary.wiley.com/doi/10.1002/cssc.201500169/abstract . This article may be used for non-commercial purposes in accordance with Wiley Terms and Conditions for Self-Archiving."

The final publication is available by subscription only.

DOI: 10.1002/cssc.201500169

© 2015 WILEY-VCH Verlag GmbH & Co. KGaA, Weinheim

Please note that any alterations made during the publishing process may not appear in this version.

Heterojunction Solar Cells Based on Silicon and Composite Films of Graphene Oxide and Carbon Nanotubes

LePing Yu, Daniel Tune, Cameron Shearer and Joseph Shapter*[a]

Abstract: Graphene oxide (GO) sheets have been used as the surfactant to disperse single walled carbon nanotubes (CNT) in water to prepare GO/CNT electrodes which are applied on silicon to form a heterojunction which can be used in solar cells. GO/CNT films with different ratios of the two components and with various thicknesses have been used as semitransparent electrodes and the influence of both factors on solar cell performance has been studied. The degradation rate of the GO/CNT-silicon devices in ambient conditions has also been explored. The influence of the film thickness on device performance is found to be related to the interplay of two competing factors, namely the sheet resistance and transmittance. CNTs help to improve the conductivity of the GO/CNT film while GO is able to protect the silicon from oxidation in the atmosphere.

Introduction

Carbon nanotube silicon heterojunction solar cells (CNT-Si) have been considered a potential replacement for current commercial crystalline silicon solar panels since they were initially reported in 2007 by Wei [1]. Since then, due to their considerable photovoltaic conversion efficiency, use of relatively simple, potentially inexpensive materials and an easy fabrication process, CNT-Si solar cells have been investigated widely [2]. So far, the highest efficiency reported has reached 15 % by doping of the CNT using H_2O_2 and HNO_3 and the addition of titanium dioxide as an antireflection layer, which is solid evidence that CNT-Si devices could be a possible substitute for traditional silicon solar cells [3]. The typical Si-CNT device is similar to a conventional n-type silicon solar cell, where a highly transparent CNT film is used to replace the expensive p-type silicon layer and front-side metallization [1, 2b-i, 2k-m]. Photon energy from the incident light can easily reach and be absorbed by the silicon leading to the creation of electron-hole pairs which then migrate to the depletion region where they are separated under the influence of 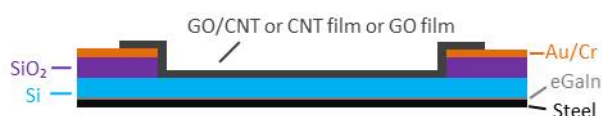the built-in potential that is the result of Fermi level equilibration across the Si-CNT heterojunction. The separated electrons and holes are collected and act as the majority charge carriers in the silicon base and the CNT film, respectively [2g].

Although CNTs have shown great potential in working as the transparent electrode, pristine CNTs are hydrophobic and thus it is a challenging task to prepare a well-dispersed CNT solution due to the strong van der Waals interactions existing between the carbon nanotubes [4]. The well-dispersed CNTs with smaller bundle sizes have better electrical properties. Two approaches, including covalent [5] and non-covalent [6] modification, are normally used to disperse CNTs. The non-covalent method can maintain the electronic structure of CNTs as well as improve the suspendability [4c] based on different bifunctional materials, including polymers [7], biomolecules [8] and surfactants [9]. The addition of surfactants, including both ionic [10] and nonionic [11] varieties, improves the dispersion of CNTs in water [12]. This is achieved by sonication of the CNTs, which produces enough mechanical energy to overcome the van der Waals interaction between the CNT bundles so that the application of the proper surfactant adsorbs onto the CNT surface and stabilizes the CNT aqueous solution by steric exclusion or electrostatic repulsion [13]. However, the nonconductive surfactants are usually difficult to rinse away completely after the formation of the CNT film [14]. Thus, the conductivity of the resulting CNT film is limited due to hindered charge transfer between individual nanotubes [15].

Recently, some researchers have starting using graphene oxide (GO) to improve the suspendability of CNTs. GO is an inexpensive precursor for large-scale production of graphene [16], and it can be prepared by mechanical exfoliation of oxidized graphite [17]. One GO sheet can have regions with two distinct characteristics in a random distribution: hydrophilic areas (such as carboxylic acid groups) and hydrophobic parts (such as aromatic benzene rings) [17]. This structure gives the GO sheets amphiphilic properties [18]. The hydrophilic parts enable GO sheets to be dissolved in water while the aromatic areas provide the ability of dispersing other hydrophobic molecules or materials, such as CNT, conducting polymers and organic semiconductors by π-π interactions [19]. Compared to the traditional surfactants, GO may lead to the creation of a more stable CNT dispersion in water [20]. Specifically, GO colloids can withstand centrifugation at high speed and be stable after controlled chemical reduction [19b]. Recently, the use of GO as the surfactant to disperse CNT has been applied in the electrode preparation of high performance supercapacitors [21] and dye sensitized solar cells [22].

Here, we explored the application of a composite of GO and CNT (GO/CNT) as the electrode with silicon to form the heterojunction in solar cells. The cell structure is shown in Figure 1. The impact of the composition of the hybrid electrode and its thickness on both efficiency and stability was studied.

[a]   Professor Joseph G. Shapter
       Centre for Nanoscale Science and Technology
       Flinders University
       Bedford Park, South Australia 5042
       E-mail: Joe.Shapter@flinders.edu.au

       Supporting information for this article is given via a link at the end of the document.

Figure 1. Schematic structure of GO/CNT-Si and CNT-Si heterojunction solar cells

Results and Discussion
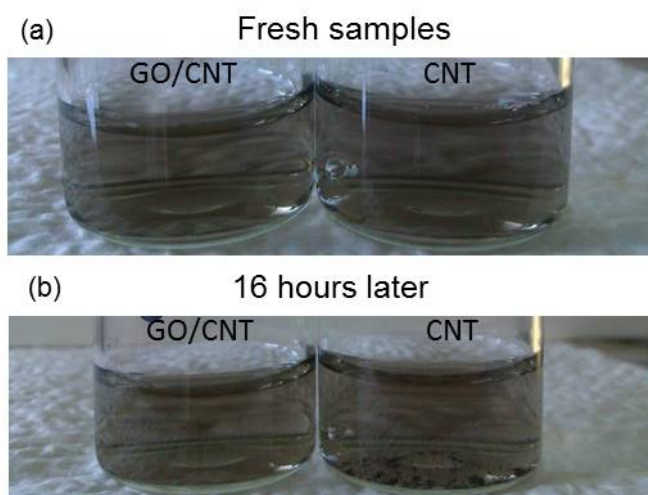
Figure 2. Comparison between the optical images of suspensions after centrifugation (GO : CNT = 1 : 2.25 and pure CNT): (a) fresh suspensions and (b) suspensions after 16 hours. Note the solid CNTs in the bottom of the vial on the right after 16 hours.

The suspension of GO : CNT = 1 : 2.25 and pure CNT were prepared and the optical images of these 2 suspension at 0 and 16 hours after centrifugation are shown in Figure 2. For fresh samples, both GO/CNT and pure CNT suspensions are clear and there is no precipitation of the material at bottom of the vial, as shown in Figure 2 (a). However, after 16 hours, there is some sediment at the bottom of the vial containing pure CNT suspension (Figure 2 (b)). This is probably caused by the strong van der Waals interactions between CNTs, and as a result, large CNT bundles are formed and fall out of the suspension [4c]. On the contrary, the suspension of GO/CNT is still clear, which indicates that GO is acting as a surfactant and does help the CNTs suspend in water.

Figure 3 shows the SEM images of five different types of electrodes at two magnifications to study the morphology of the electrode materials. GO sheets can be observed in Figure S2 which shows the SEM images of the dried GO and GO/CNT drops on silicon wafer from the supernatants after centrifugation and these images indicate that there are still some GO sheets after high speed centrifugation in the suspension. As shown in Figure 3 (a), the SEM image of pure GO film shows the typical wrinkled morphology of GO sheets. There are plenty of overlapping regions between different GO sheets and these GO sheets form a continuous network across the whole film. Figure
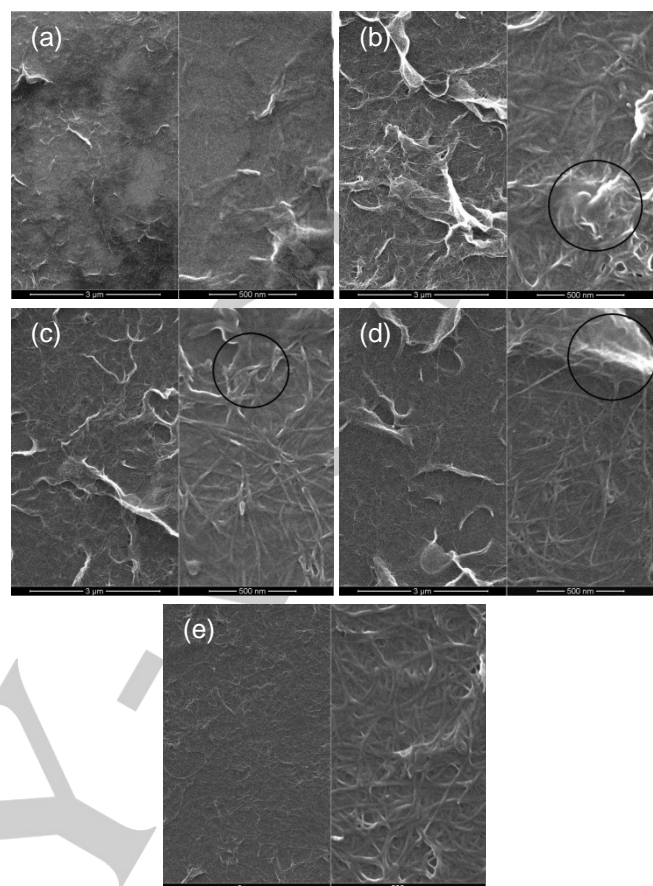
Figure 3. SEM images of electrodes on silicon at 2 magnifications (left side: X 40000 and right side: X 160000): (a) pure GO; (b) GO : CNT = 2.25 : 1; (c) GO : CNT = 1 : 1; (d) GO : CNT = 1 : 2.25 and (e) pure CNT. The dark circles are used to point out the position of GO sheets on electrodes. The optical transmittances of all these films are about 60 %, as shown in Figure S1.

3 (b), (c) and (d) show the SEM images of GO/CNT electrode films with different ratios of GO : CNT. Many wrinkles are observed on these images at low magnification (X 40000) and they are due to the presence of GO sheets. The fact that these wrinkles are different from the ones on pure GO electrode is a result of the GO sheets being separated and unable to stack together after introducing CNTs into the electrode system. Similarly, the wrinkles of the GO sheets on GO/CNT electrodes look rougher than those on pure GO electrodes, which is also possibly the result of various stacking arrangements during vacuum filtration. In comparison, the pure CNT electrode shows only the familiar randomly aligned features of CNTs (Figure 3 (e)).
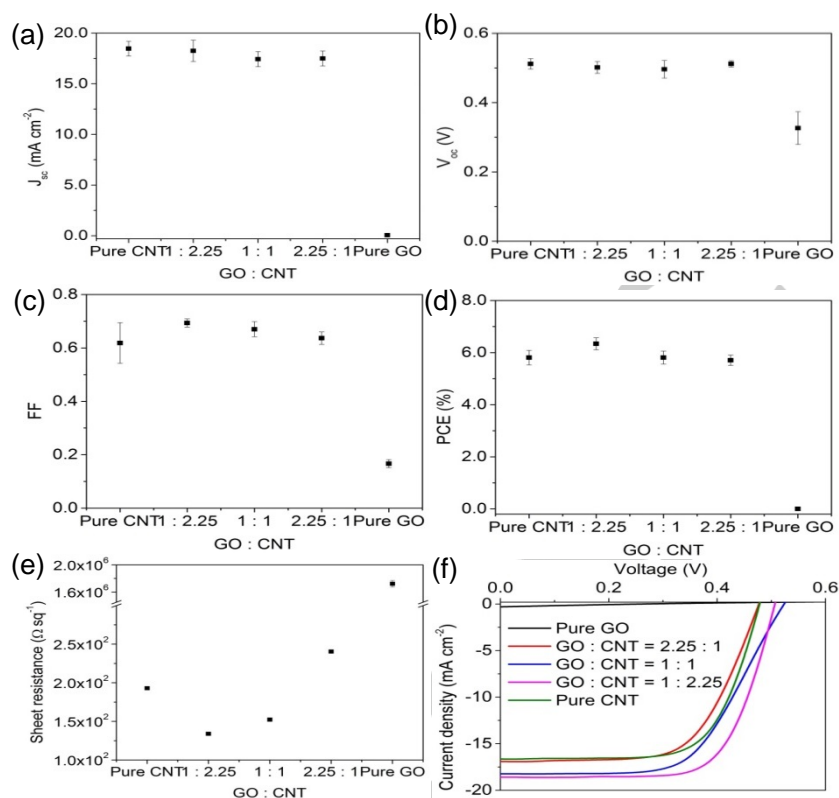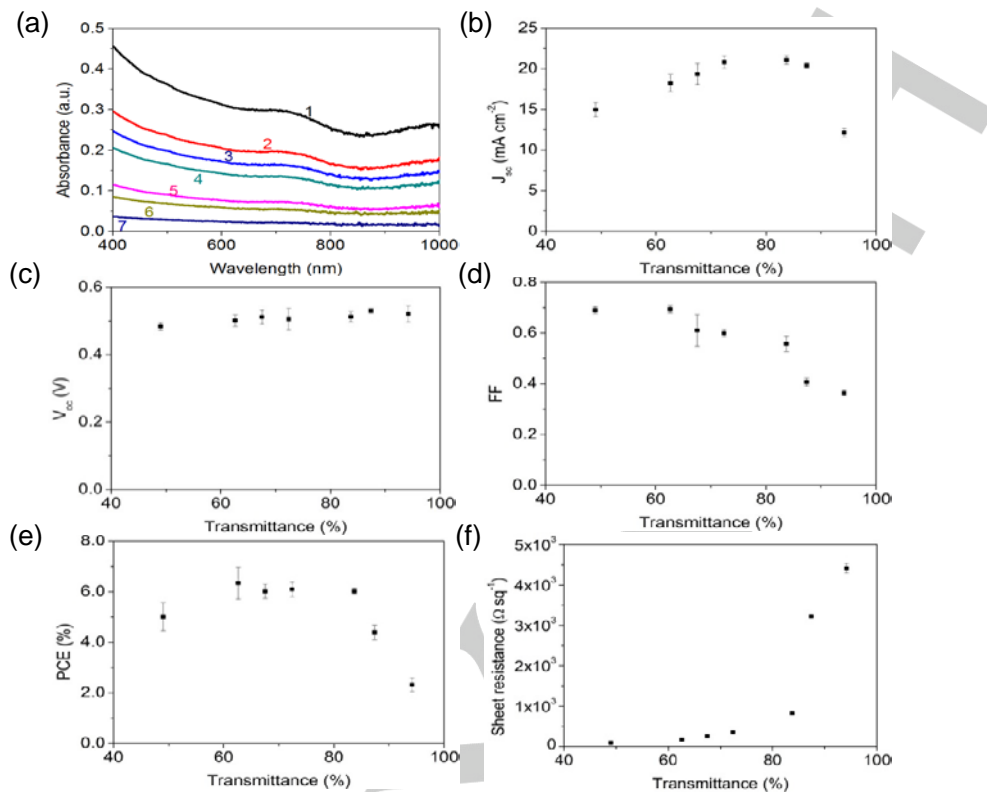
Figure 4. The performance of the GO/CNT devices with different ratios of components, pure GO and pure CNT devices: (a) J_{sc}; (b) V_{oc}; (c) FF and (d) PCE; (e) the sheet resistance of the GO/CNT films and (f) typical J-V curves of 5 different types of devices. The optical transmittances of all films were 60 %.

GO : CNT Ratio	J_{SC}	V_{OC}	FF	PCE	Sheet resistance
	mA cm^{-2}	V		%	Ω sq^{-1}
Pure CNT	18.5 ± 0.73	0.51 ± 0.02	0.62 ± 0.08	5.81 ± 0.28	193.06 ± 0.05
1:2.25	18.2 ± 1.06	0.50 ± 0.02	0.69 ± 0.02	6.34 ± 0.23	134.02 ± 0.04
1:1	17.4 ± 0.74	0.50 ± 0.03	0.67 ± 0.03	5.81 ± 0.25	152.26 ± 0.05
2.25 : 1	17.5 ± 0.73	0.51 ± 0.01	0.64 ± 0.02	5.71 ± 0.20	240.52 ± 0.04
Pure GO	0.06±0.019	0.33 ± 0.05	0.17 ± 0.02	0.00 ± 0	1.72 x 10^6 ± 4.88 x 10^4

In order to study the influence of the amount of the GO in the electrode, GO/CNT electrodes with various ratios of GO and CNT have been prepared. Raman microspectrophotometric characterization of the electrodes is provided in Figures S3 and S4. These electrodes are then used to make carbon nanomaterial-Si solar cells. Once formed the electrode is subject to three treatments. Initially, a HF treatment is used to remove the silicon oxide layer followed by a SOCl$_2$ treatment to improve the conductivity of the nanotubes through a shift in the Fermi level. Finally another HF treatment removes any residue oxide reformed during the second treatment.

Nanotubes exposed to air are naturally p-type due to adsorption of O$_2$. When brought into close contact with the n-type silicon, a heterojunction is established. Photons are absorbed by the silicon creating excitons which diffuse to the depletion region created and are separated there to provide the observed current. The treatments of the GO/CNT layers are each quite important. During the deposition of the carbon layer, a thick silicon oxide layer grows at the interface between the silicon and the carbon layer. The first HF treatment is used to remove this oxide to ensure the formation of an effective heterojunction. SOCl$_2$ treatment is used to remove electrons from the valance band of the nanotubes. The effect of this treatment is to improve the conductivity of the nanotubes in the electrode and enhance solar cell performance. A final HF treatment removes any traces of oxide to give the ultimate photovoltaic performance.

Figure 5. (a) The optical absorbance spectra of GO/CNT films with transmittance of (1) 94.5 %, (2) 87.4 %, (3) 83.7 %, (4) 72.4 %, (5) 67.5 %, (6) 62.6 % and (7) 49.0 %; and the performance of the GO/CNT (GO : CNT = 1 : 2.25) devices with different thickness of GO/CNT films: (b) J_{sc}; (c) V_{oc}; (d) FF and (e) PCE; (f) the sheet resistance of the GO/CNT films.

Figure 4 shows some vital photovoltaic parameters and the J-V curves of GO/CNT devices using different ratios of materials in the composites, including short circuit current density (J_{sc}), open circuit voltage (V_{oc}), fill factor (FF) and power conversion efficiency (PCE). In terms of J_{sc}, V_{oc}, and FF, the cells with pure GO electrodes show the worst performance, especially the extremely low J_{sc} (approximately 0.06 mA cm^{-2}). Both the J_{sc} and V_{oc} of the other four types of device are very similar. The FF increased slightly as the ratio of CNTs in the composite was increased; however the FF of cells with pure CNT films was cells with the other two ratios and to the pure CNT films, while the cells with pure GO electrodes exhibited the worst performance among these devices. This can be explained in reference to the sheet resistance of these films. As a result, GO/CNT (1 : 2.25) devices displayed better performance compared to the (1 : 2.25) films had the lowest sheet resistance (approximate 130 Ω sq^{-1}) after all three treatments while the GO/CNT (2.25 : 1) film had the highest value (approximate 240 Ω sq^{-1}). Thus, the GO/CNT (1 : 2.25) film is the most conductive and this helps to maintain charge separation, which leads to a higher FF and therefore PCE. This is also consistent with the fact that GO on its own is not very conductive [23] and the sheet resistance of the GO films used here are in the order of 10^6 Ohms sq^{-1}. As the amount of GO is increased in the GO/CNT, the electrode becomes less conductive with the same transmittance though slight amount of GO seems to help to reduce the sheet

resistance of the electrode, as shown in Figure 4 (e). This improvement in resistance leads to a marginal improvement in PCE.

GO/CNT films (GO : CNT = 1 : 2.25) of different thickness were incorporated into solar cells to investigate the influence of thickness on performance, as shown in Figure 5 (a). In Figure 5 (b), it can be seen that as the thickness of the film decreases (and the transmittance and sheet resistance increase), the J_{sc} increases until a peak at approximately 80 % transmittance then there is a sharp decrease of J_{sc} for very thin films. However, it can be seen in Figure 5 (c) that V_{oc} is quite stable for all the GO/CNT film thicknesses, but there is a general decrease in FF seen in Figure 5 (d) as the films become thinner. As a result, the PCE of the devices, shown in Figure 5 (e), increases as the GO/CNT films become thinner, then plateau from 60 % to 85 % transmittance and then sharply decreases for very thin films. The plateau region (to 85 %) is slightly broader at high transmittance region than that of CNT only device (to about 80 %) [2I]. This trend is related to two factors, namely, the transmittance and sheet resistance of the GO/CNT electrodes. Thinner films absorb fewer photons, as shown in Figure 5 (a), and thus more photon energy can pass through and be absorbed in the silicon which produces excitons. However, as shown in Figure 5 (f), the sheet resistance of thinner films (approximately 4500 Ω sq^{-1} for
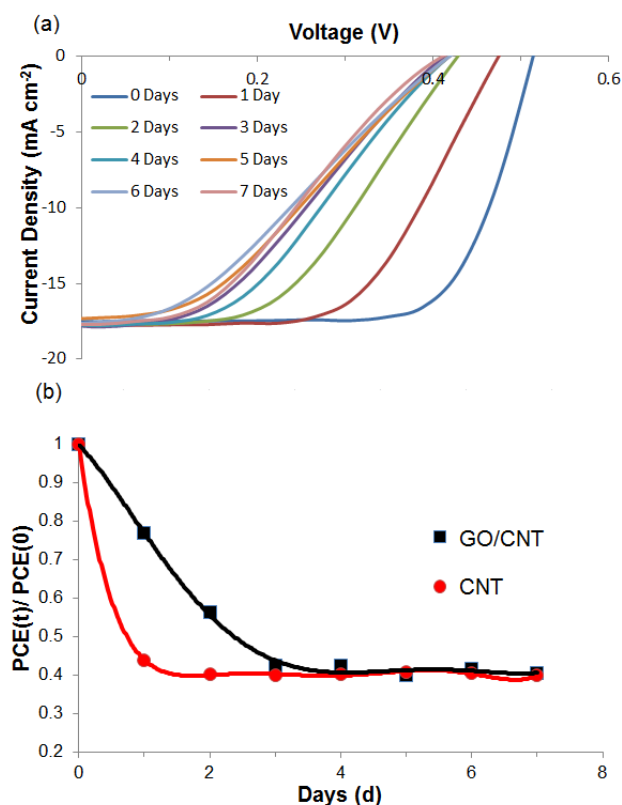
Figure 6. The degradation of the devices (a) current density-voltage curves of GO/CNT device over seven days and (b) comparison between GO/CNT (GO : CNT = 1 : 2.25; 60 % transmittance) and CNT cells. Lines added to guide the eye.

95 % transmittance) is considerably higher than that of thicker films (approximately 100 Ω sq^{-1} for 50 % transmittance), which is caused by the fact that the sparse GO/CNT network contains fewer charge percolation pathways. Transmittance is used to characterize film thicknesses as it given the best representation of the number of photons that reach the active element in the cell, namely the silicon.

To investigate the stability of the photovoltaic response of the cells, J-V curves were completed daily over 1 week with the cells left in ambient conditions. As shown in Figure 6, the PCE of devices with both GO/CNT (GO : CNT = 1 : 2.25; 60 % transmittance) and pure CNT electrodes decreased within first three days and then remained stable for a further week. The performance of the device with pure CNT electrode decayed much more dramatically during the first day, as shown in Figure 6 (b). The main reason for the decrease of PCEs is due to the reduction in FF (as shown in Figure S5 (a)). There are 2 potential reasons for the degradation, including the growth of an oxide layer on the silicon surface and an increase in the sheet resistance, which is mainly related to how long the doping effect of SOCl$_2$ treatment lasts. Here, since the increase of the sheet

resistance (of both pure CNT and GO/CNT films) is very limited (about 10 %) during 7 days (as shown in Figure S5 (b)), the main reason for the degradation of the performance must be the growth of an insulating oxide layer, which serves to hinder the transport of photogenerated holes from silicon to pure CNT and GO/CNT films after exciton dissociation. This leads to a drastic decrease in FF (0.71 to 0.36), accompanied by a marginal reduction in V_{oc} (0.51 to 0.43 V). Thus, the faster degradation of the CNT cells compared to GO/CNT devices may indicate that the GO sheets can hinder oxygen in the atmosphere from reaching the silicon surface and hence slow the formation of the oxide to some degree. As such, the GO has the dual benefit of making more stable dispersions to help with electrode production as well as improving the device stability but these benefits are offset by a lower of electrode conductivity meaning that the overall photovoltaic efficiencies do not change dramatically with the GO:CNT ratio.

In an attempt to overcome the limited conductivity of the GO/CNT electrodes, heat treatment was used to reduce GO to graphene, as this has been shown to increase the conductivity of GO films [24]. However, after heat treatment, reduced graphene oxide absorbs significantly more light than GO does, as shown in Figure S6, and the efficiencies of the cell with limited transmittance films working as the electrode are always poor due to the reduced photon energy absorbed by the Si substrates [2l]. Recently it has been shown that some conducting polymers can be used to build a better depletion region at the heterojunction [2j, 25]. This approach could be used to fabricate new composites (with GO, CNTs and conducting polymers) which can then be used as electrodes. In terms of the stability improvement, polymer antireflection layers, such as PDMS, are some of the easiest and most effective approaches [2h]. Although there are still many challenges before possible industrial application, GO/CNT silicon heterojunction solar cells are a promising alternative with potentially lower cost compared to conventionally fabricated silicon solar panels.

Conclusions

GO was used as a surfactant to disperse CNTs in water and produce a stable suspension and then to form a GO/CNT film which was used as a semitransparent electrode on silicon to establish a heterojunction solar cell. Adding a small amount of GO to CNTs improved the properties of the electrode and thus the performance of the solar cells. GO/CNT films with different constituent ratios were investigated and it was observed that the performance of the devices increased as the amount of CNT increased in the composite electrode, due to a decrease in the sheet resistance of the films at the same transmittance. As with CNT-Si solar cells, the performance of GO/CNT-Si devices is clearly related to the film thickness, which determines both the amount of light penetrating through to the silicon as well as the sheet resistance of the electrode, and GO/CNT films with

transmittances ranging from 60 to 85 % led to the best performances in this study. Importantly, compared to CNT only devices, it appears that the incorporation of GO into film can increase the stability of the cell to some degree. The improved dispersions provided by the GO may allow the production of devices with larger active areas which will be important for future research.

Experimental Section

In order to collect the GO solids, 5 mg mL^{-1} commercial GO in ethanol (Graphene Supermarket, USA) was exposed to ambient atmosphere to allow the evaporation of the solvent. The GO solids were then dispersed in water with bath sonication at room temperature for 30 min to prepare the GO stock solution with a concentration of 0.2 mg mL^{-1}. The GO solution was then added to the suspension of CNT (P3-SWNT, Carbon Solutions Inc., USA) in water, and the mixture was sonicated for 2 h to form the GO/CNT suspension in water with 3 different weight ratios (GO : CNT = 2.25 : 1, 1 : 1 and 1 : 2.25). In order to remove large agglomerates of GO and CNT, the solutions were centrifuged for 1 h at 17500 g. The residues at the bottom were discarded and the supernatant were further centrifuged in the identical manner. The second supernatant was collected to prepare the GO/CNT electrodes in the following sections.

GO/CNT electrodes were prepared by vacuum filtration[22]. In order to explore the effects of GO/CNT electrode thickness, different volumes (50, 100, 200, 300, 400, 500 and 800 µL) of GO/CNT (GO : CNT = 1 : 2.25) suspension were diluted with water to 250 mL in total. The GO and CNT in the dilution were collected on a 'target' mixed cellulose ester membrane (MCE, 0.45 µm, HAWP, Millipore, Australia) with the help of a 'stencil' nitrocellulose membrane (25 nm, VSWP, Millipore, Australia) with four holes (0.49 cm^2 each). Since 'target' and 'stencil' membrane have different pore size, this leads to a faster flow rate at the regions of four holes and four identical membranes can be collected in one filtration on MCE. The central areas of the GO/CNT membrane were cut out of the MCE for device fabrication as well as optical and electrical properties testing. 750 µL (GO : CNT = 1 : 1) and 800 µL (GO : CNT = 2.25 : 1) of GO/CNT suspension were diluted and filtered in the same manner to compare the ratio impact at 60 % transmittance. In order to prepare the pure CNT electrode, 800 µL pure SWCNT suspension after centrifugation was diluted in 250 mL with water and the same vacuum filtration steps were conducted.[2j, 2l, 2m]

Phosphorous doped n-type silicon wafers (5-10 Ω cm, 525 µm thick with a 100 nm thermal oxide, ABC GmbH, Germany) were used as the substrates for devices. Positive photoresist (AZ1518, micro resist technology GmbH, Munich, Germany) was applied on wafers by a spin-coater at 3000 rpm for 30 s. The wafers with photoresist were baked at 100 °C for 1 min. A mask was used to define the active area (0.079 cm^2) of the device on the wafer by exposure to UV light for 5 min. By immersing the wafer in a developer solution (AZ 326 MIF, AZ electronic Materials, GmbH, Munich, Germany) for 1 min, the reacted photoresist was dissolved and the pattern of the active area remained on the wafer. The chromium/gold front electrode (Cr/Au, 5/145 nm) was applied to the wafer by a sputter coater (Q300T-D) with thickness controlled by a quartz crystal microbalance. The silicon was then immersed in acetone for 30 min to dissolve the photoresist. A drop of buffered oxide etch (BOE, 6:1 of 40% NH_4F and 49% hydrofluoric acid (HF), Sigma-Aldrich, Australia) was applied to the central area to remove the front thermal oxide layer. The GO/CNT/MCE membranes were applied on the substrate with GO/CNT side down. A drop of water was put on top and the device was clamped and baked for 20 min at 80 °C. Following cooling

to room temperature over 12 h, 3 x 30 min acetone washes were done to dissolve the MCE film. After scratching of the rear silicon oxide layer, the device was mounted on stainless steel with gallium indium eutectic (eGaIn). The resulting device is referred to as 'as-prepared', as shown in Figure 1. In order to evaluate the optical (transmittance) and electrical (sheet resistance) properties, GO/CNT/MCE films were applied on microscope slides and MCE membranes were dissolved by acetone in the identical manner.

For all devices, there are 3 post treatments. Firstly, in order to etch the silicon oxide layer formed in the device fabrication, a drop of HF (2 %) was applied on the active area for 10 s, followed by rinsing with water, ethanol and blow drying with N_2. HCl, instead of HF, was applied in a same manner on the microscope slides to avoid reaction between HF and the glass. Secondly, a drop of $SOCl_2$ was applied to GO/CNT films on microscope slides or solar cells before rinsing with ethanol and drying with N_2, which improves the conductivity of the GO/CNT film by shifting the Fermi level of the CNTs into the valence band and reducing resistance at the tube-tube junctions [2d]. Finally, a second HF treatment was conducted to remove the silicon oxide layer formed during $SOCl_2$ treatment, in the same manner as the previous one. In order to reduce GO to graphene, heat treatment of GO/CNT films was conducted at 300 °C under Ar and H_2 atmosphere for 2 h [24].

The performance (current density-voltage curves) of the devices was evaluated by a custom Labview^{TM} virtual instrument with a Keithley 2400 source unit. The power density of the collimated xenon-arc light at the cell plane was calibrated to 100 mW cm^{-2} by a standard test silicon cell (PV Measurements, NIST-traceable certification) and the light source was passed through an AM 1.5G filter. The sheet resistance of the GO/CNT films on microscope slides was determined by a four point probe (Keithink). The transmittance of the GO/CNT was calculated by averaging the transmittance values at two wavelengths (450 and 850 nm) in UV-Vis-NIR spectra with a vacant slide for background subtraction. The morphology of the GO/CNT electrode was determined by both atomic force microscope (AFM) (Nanoscope, Multimode, Bruker) and scanning electron microscope (SEM) (Inspect F50, FEI).

[1] J. Q. Wei, Y. Jia, Q. K. Shu, Z. Y. Gu, K. L. Wang, D. M. Zhuang, G. Zhang, Z. C. Wang, J. B. Luo, A. Y. Cao, D. H. Wu, *Nano Lett.* **2007**, *7*, 2317-2321.

[2] a) D. D. Tune, B. S. Flavel, R. Krupke, J. G. Shapter, *Adv. Energy Mater.* **2012**, *2*, 1043-1055; b) A. Behnam, J. L. Johnson, Y. Choi, M. G. n. Ertosun, A. K. Okyay, P. Kapur, K. C. Saraswat, A. Ural, *Appl. Phys. Lett.* **2008**, *92*, 243116; c) Y. Jia, J. Wei, K. Wang, A. Cao, Q. Shu, X. Gui, Y. Zhu, D. Zhuang, G. Zhang, B. Ma, L. Wang, W. Liu, Z. Wang, J. Luo, D. Wu, *Adv. Mater.* **2008**, *20*, 4594-4598; d) Z. Li, V. P. Kunets, V. Saini, Y. Xu, E. Dervishi, G. J. Salamo, A. R. Biris, A. S. Biris, *Appl. Phys. Lett.* **2008**, *93*, 243117; e) Y. Jia, P. X. Li, J. Q. Wei, A. Y. Cao, K. L. Wang, C. L. Li, D. M. Zhuang, H. W. Zhu, D. H. Wu, *Mater. Res. Bull.* **2010**, *45*, 1401-1405; f) P. Wadhwa, B. Liu, M. A. McCarthy, Z. C. Wu,

A. G. Rinzler, *Nano Lett.* **2010**, *10*, 5001-5005; g) Y. Jia, A. Y. Cao, X. Bai, Z. Li, L. H. Zhang, N. Guo, J. Q. Wei, K. L. Wang, H. W. Zhu, D. H. Wu, P. M. Ajayan, *Nano Lett.* **2011**, *11*, 1901-1905; h) Y. Jia, P. Li, X. Gui, J. Wei, K. Wang, H. Zhu, D. Wu, L. Zhang, A. Cao, Y. Xu, *Appl. Phys. Lett.* **2011**, *98*, 133115; i) Y. Jia, A. Y. Cao, F. Y. Kang, P. X. Li, X. C. Gui, L. H. Zhang, E. Z. Shi, J. Q. Wei, K. L. Wang, H. W. Zhu, D. H. Wu, *Phys. Chem. Chem. Phys.* **2012**, *14*, 8391-8396; j) D. D. Tune, B. S. Flavel, J. S. Quinton, A. V. Ellis, J. G. Shapter, *ChemSusChem* **2013**, *6*, 320-327; k) D. D. Tune, F. Hennrich, S. Dehm, M. F. G. Klein, K. Glaser, A. Colsmann, J. G. Shapter, U. Lemmer, M. M. Kappes, R. Krupke, B. S. Flavel, *Adv. Energy Mater.* **2013**, *3*, 1091-1097; l) D. D. Tune, J. G. Shapter, *Nanomaterials* **2013**, *3*, 655-673; m) D. D. Tune, A. J. Blanch, R. Krupke, B. S. Flavel, J. G. Shapter, *Phys. Status Solidi A* **2014**, *211*, 1479-1487.

[3] E. Z. Shi, L. H. Zhang, Z. Li, P. X. Li, Y. Y. Shang, Y. Jia, J. Q. Wei, K. L. Wang, H. W. Zhu, D. H. Wu, S. Zhang, A. Y. Cao, *Sci Rep* **2012**, *2: 884*.

[4] a) R. Rastogi, R. Kaushal, S. K. Tripathi, A. L. Sharma, I. Kaur, L. M. Bharadwaj, *Journal of Colloid and Interface Science* **2008**, *328*, 421-428; b) S. W. Lee, B. S. Kim, S. Chen, Y. Shao-Horn, P. T. Hammond, *Journal of the American Chemical Society* **2009**, *131*, 671-679; c) J. K. Sprafke, S. D. Stranks, J. H. Warner, R. J. Nicholas, H. L. Anderson, *Angew. Chem. Int. Ed.* **2011**, *50*, 2313-2316.

[5] M. Sathiya, A. S. Prakash, K. Ramesha, J. M. Tarascon, A. K. Shukla, *Journal of the American Chemical Society* **2011**, *133*, 16291-16299.

[6] X. L. Li, Y. J. Qin, S. T. Picraux, Z. X. Guo, *Journal of Materials Chemistry* **2011**, *21*, 7527-7547.

[7] M. Noked, S. Okashy, T. Zimrin, D. Aurbach, *Angew. Chem. Int. Ed.* **2012**, *51*, 1568-1571.

[8] a) S. S. Bale, P. Asuri, S. S. Karajanagi, J. S. Dordick, R. S. Kane, *Adv. Mater.* **2007**, *19*, 3167-3170; b) X. G. Han, Y. L. Li, Z. X. Deng, *Adv. Mater.* **2007**, *19*, 1518-1522.

[9] J. Rausch, R. C. Zhuang, E. Mader, *Journal of Applied Polymer Science* **2010**, *117*, 2583-2590.

[10] Z. Sun, V. Nicolosi, D. Rickard, S. D. Bergin, D. Aherne, J. N. Coleman, *Journal of Physical Chemistry C* **2008**, *112*, 10692-10699.

[11] a) V. C. Moore, M. S. Strano, E. H. Haroz, R. H. Hauge, R. E. Smalley, J. Schmidt, Y. Talmon, *Nano Lett.* **2003**, *3*, 1379-1382; b) W. Wenseleers, Vlasov, II, E. Goovaerts, E. D. Obraztsova, A. S. Lobach, A. Bouwen, *Adv. Funct. Mater.* **2004**, *14*, 1105-1112.

[12] E. E. Tkalya, M. Ghislandi, G. de With, C. E. Koning, *Curr. Opin. Colloid Interface Sci.* **2012**, *17*, 225-231.

[13] M. S. Strano, V. C. Moore, M. K. Miller, M. J. Allen, E. H. Haroz, C. Kittrell, R. H. Hauge, R. E. Smalley, *J. Nanosci. Nanotechnol.* **2003**, *3*, 81-86.

[14] H. Z. Geng, K. K. Kim, K. P. So, Y. S. Lee, Y. Chang, Y. H. Lee, *Journal of the American Chemical Society* **2007**, *129*, 7758-7759.

[15] L. B. Hu, J. W. Choi, Y. Yang, S. Jeong, F. La Mantia, L. F. Cui, Y. Cui, *Proceedings of the National Academy of Sciences of the United States of America* **2009**, *106*, 21490-21494.

[16] a) S. Park, R. S. Ruoff, *Nature Nanotechnology* **2009**, *4*, 217-224; b) M. J. Allen, V. C. Tung, R. B. Kaner, *Chem. Rev.* **2010**, *110*, 132-145.

[17] D. R. Dreyer, S. Park, C. W. Bielawski, R. S. Ruoff, *Chemical Society Reviews* **2010**, *39*, 228-240.

[18] Y. Cao, J. Zhang, J. Feng, P. Wu, *ACS Nano* **2011**, *5*, 5920-5927.

[19] a) L. Qiu, X. Yang, X. Gou, W. Yang, Z.-F. Ma, G. G. Wallace, D. Li, *Chemistry-a European Journal* **2010**, *16*, 10653-10658; b) J. Y. Luo, L. J. Cote, V. C. Tung, A. T. L. Tan, P. E. Goins, J. S. Wu, J. X. Huang, *Journal of the American Chemical Society* **2010**, *132*, 17667-17669.

[20] L. J. Cote, J. Kim, V. C. Tung, J. Y. Luo, F. Kim, J. X. Huang, *Pure Appl. Chem.* **2011**, *83*, 95-110.

[21] B. You, N. Li, H. Zhu, X. Zhu, J. Yang, *ChemSusChem* **2013**, *6*, 474-480.

[22] J. Ma, L. Zhou, C. Li, J. Yang, T. Meng, H. Zhou, M. Yang, F. Yu, J. Chen, *Journal of Power Sources* **2014**, *247*, 999-1004.

[23] S. F. Pei, J. P. Zhao, J. H. Du, W. C. Ren, H. M. Cheng, *Carbon* **2010**, *48*, 4466-4474.

[24] X. F. Gao, J. Jang, S. Nagase, *Journal of Physical Chemistry C* **2010**, *114*, 832-842.

[25] L. P. Yu, D. D. Tune, C. J. Shearer, J. G. Shapter, *ChemNanoMat*, DOI: 10.1002/cnma.201400005.

Entry for the Table of Contents (Please choose one layout)

Layout 1:

FULL PAPER

Graphene oxide (GO) sheets have been used as the surfactant to disperse single walled carbon nanotubes (CNT) in water to prepare GO/CNT electrodes which are applied on silicon to form a heterojunction which can be used in solar cells.
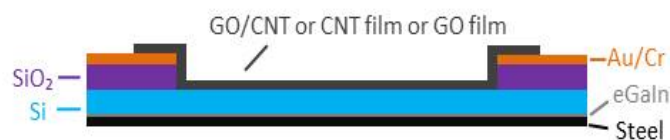
LePing Yu, Daniel Tune, Cameron Shearer and Joseph Shapter*

Page No. – Page No.

Title